

Refractive index dependence of the absorption and emission cross sections at 1.54 μm of Er^{3+} coupled to Si nanoclusters

N. Daldosso,^{a)} D. Navarro-Urrios, M. Melchiorri, and L. Pavesi
 Dipartimento di Fisica, Università di Trento, Via Sommarive 14, I-38050 Povo (Trento), Italy

C. Sada
 INFN-MATIS Dipartimento di Fisica, Università di Padova, Via Marzolo 8, I-35131 Padova, Italy

F. Gourbilleau and R. Rizk
 SIFCOM, UMR CNRS 6176, ENSICAEN, 6 Boulevard Maréchal Juin, 14050 CAEN, France

(Received 16 November 2005; accepted 20 March 2006; published online 17 April 2006)

Absorption coefficient (α_{abs}) of Er^{3+} ions coupled to Si nanoclusters (Si-nc) in SiO_2 has been determined by optical transmission measurements in rib-loaded waveguides characterized by different refractive indices, thus gauging an Er^{3+} absorption cross section (σ_{abs}) of $0.4\text{--}1.2 \times 10^{-20} \text{ cm}^2$ at 1534 nm. Although no significant enhancement due to the presence of Si-nc was observed, a clear dependence on the refractive index has been found. Measurements of the decay lifetime permit one to model the behavior as due to both local and mean field variations caused by the composite nature of the core waveguide layer. © 2006 American Institute of Physics.

[DOI: 10.1063/1.2195773]

Integrated erbium-doped waveguide amplifiers (EDWAs) could become fundamental elements in planar lightwave circuits allowing a regeneration of the propagating signal within short distances thanks to the possibility of being compact, cheap, and integrated on silicon. The use of broadband efficient sensitizers for Er^{3+} ions, such as Si nanoclusters (Si-nc),^{1–3} relaxes the expensive requirement for the pump source when directly exciting the Er ions at 980 or 1420 nm. This motivates the convenience of EDWA for short distances where the costs of erbium-doped fiber amplifiers are not sustainable. Si-nc in silica matrices are very efficient sensitizers for Er due to their broad absorption band in the ultraviolet-visible range, where very cheap diode lasers or light-emitting diodes are available. In fact, the Si-nc absorption cross section is orders of magnitude larger (10^{-16} cm^2 at 488 nm for low pumping power) (Ref. 4) than that of Er in SiO_2 (10^{-21} cm^2 at 980 nm).⁵ Moreover, the refractive index of silica is increased by the presence of Si-nc, thus allowing good light confinement. It is assumed that the energy transfer to Er ions takes place via carriers through an Auger-type interaction,⁶ resulting in a fast ($\sim 1 \mu\text{s}$) and a very efficient ($\sim 60\%$) Er excitation. Still under debate is whether or not the presence of Si-nc modifies the Er^{3+} absorption cross section at 1.54 μm .^{7–10}

In this letter, Si-nc coupled to Er^{3+} rib-loaded waveguides have been fabricated with various refractive index values of the core layer. Optical transmission measurements have been performed to measure propagation losses and to assess the Er^{3+} absorption cross section at 1.54 μm . Photoluminescence (PL) and lifetime decay measurements complete the analysis.

Er^{3+} coupled to Si-nc waveguides have been prepared by reactive magnetron co-sputtering of a pure silica target topped with Er_2O_3 pellets.¹¹ The mixture of hydrogen to argon, allowing the growth of silicon-rich oxide (SRO), was maintained to a rate of 60%. The Si substrates, on which a 10 μm thermal SiO_2 layer was previously grown, were not

intentionally heated during the process. After the deposition of the Er/SRO layer, a SiO_2 cladding layer has been deposited by sputtering a SiO_2 target in pure argon plasma, and the samples have then been annealed at 900 °C under pure N_2 flux for various annealing times to activate Er ions and to precipitate Si-nc. The annealing temperature was set to the value which optimizes the energy transfer among Si-nc and Er ions.¹² The annealing time was changed to study the effects of changing dielectrics with the same excess silicon content. The parameters of the processed layer were measured on slab waveguides by (i) *m*-line measurements at 632.8 nm to get the refractive index (*n*) and core layer thickness, and (ii) secondary ion mass spectrometry and Rutherford backscattering (RBS) to determine Er and Si, O profile concentration. Data are summarized in Table I. Then, lithography and etching were used to define rib-loaded monomode waveguides (Fig. 1, inset). Atomic force microscopy has been used to determine the etch depth and rib width of the waveguides. Er^{3+} absorption spectra have been obtained by the insertion losses technique. Light of a tunable diode laser

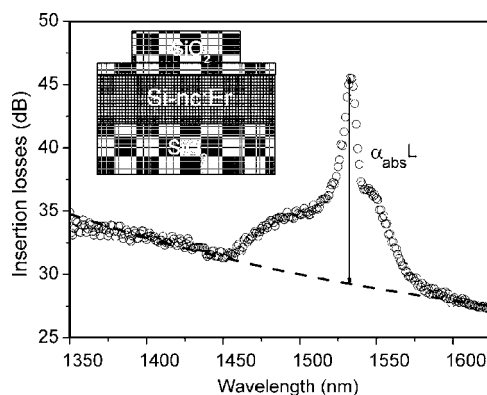


FIG. 1. Insertion losses of waveguide sample B (circles). The dashed line is an estimation of the contribution due to scattering and coupling losses and serves as baseline. The difference between the insertion loss spectrum and the baseline corresponds to the Er^{3+} absorption spectrum $\alpha_{\text{abs}}L$, where $L=3 \text{ cm}$ is the waveguide length. The inset is a cross section scheme of the waveguide structure.

^{a)}Electronic mail: daldosso@science.unit.it

TABLE I. Waveguide parameters: Annealing time, Si excess, Er content, core layer thickness, SiO₂ top cladding thickness, etch depth trough the top cladding, core-layer refractive index n at 632.8 nm, confinement factor Γ of the fundamental mode optical, and absorption losses α_{abs} at 1534 nm. Waveguides A and B have a measured rib width of about 7 μm , whereas waveguides C, D, and D⁺ have a rib width of about 12 μm .

Waveguide sample	Annealing time (min)	Si excess (at. %)	Er content ($\times 10^{20} \text{ cm}^{-3}$)	Core layer thickness (nm)	SiO ₂ top cladding thickness (nm)	Etch depth (nm)	n	Γ	α_{abs} (dB/cm)
A	240	6–7	~ 3	750	1000	900	1.61 ± 0.01	0.66 ± 0.02	3.6 ± 0.5
B	60	7	4 ± 0.1	750	1800	1600	1.545	0.51 ± 0.02	5.4 ± 0.5
C	30	7	5.4 ± 0.2	840	1000	340	1.516	0.48 ± 0.02	8.5 ± 0.7
D	10	7	5.4 ± 0.2	840	1000	310	1.48 ± 0.01	0.28 ± 0.03	7.5 ± 0.5
D ⁺	10	7	5.4 ± 0.2	840	790	310	1.48 ± 0.01	0.20 ± 0.03	6.9 ± 0.4

(1350–1630 nm; 4 mW) was coupled into the waveguide through a single-mode tapered fiber moved by a piezoelectric stage. The transmitted light was simultaneously observed by an InGaAs camera and measured by a Ge detector through suitable optics. Lifetimes were extracted from luminescence decay measurements at low photon flux.

The effect of the annealing time on n is reported in Table I: The longer the annealing, the higher n which suggests an increased Si clustering,¹³ according to a more complete phase separation between Si and SiO₂. This is confirmed by Bruggeman calculations of n : for 240 min of annealing, Si-nc in SiO₂ well reproduce the experimental values; on the contrary, for lower annealing time, a substoichiometric silica (SiO _{x}) is needed. A minor effect on n due to an increased densification of the layers is also present.

Figure 1 shows insertion loss measurements on waveguide sample B. The Er³⁺ characteristic absorption (α_{abs}) peak at 1534 nm is superimposed on a background (dashed line) which decreases with λ . The background is due to coupling (α_{coupling}) and propagation ($\alpha_{\text{propagation}}$) losses. Coupling losses can be considered constant, whereas propagation losses at long λ are mainly due to Rayleigh scattering because of the composite structure of the core layer and the waveguide roughness. From the fit of the data where Er absorption is negligible, we have determined $\alpha_{\text{propagation}}$ thus allowing the determination of α_{abs} by difference, once α_{coupling} is estimated. From α_{abs} , cross sections (σ_{abs}) can be deduced. In fact, $\alpha_{\text{abs}} = \Gamma \sigma_{\text{abs}} N_{\text{Er}}$, where Γ are the optical confinement factors of the fundamental optical mode which have been calculated from the geometry of the rib-loaded waveguides (see Table I), and N_{Er} is the Er concentration determined by RBS. Note that the σ_{abs} values are determined taking on that all Er ions are optically active. This has been experimentally confirmed by PL measurements, whose intensity has been compared with an Er:SiO₂ reference sample, under resonant (488 nm) and nonresonant (476 nm) excitation as a function of the photon flux: From the difference between the numbers of Er³⁺ ions in the excited state, the amount of Er³⁺ ions directly excited can be extracted and it corresponds to N_{Er} .¹⁴

For waveguide sample B, $\alpha_{\text{abs}} = 5.4 \text{ dB/cm}$ at 1534 nm, which corresponds to $\sigma_{\text{abs}} = 6 \pm 2 \times 10^{-21} \text{ cm}^2$. This value is very close to that of Er³⁺ in pure silica ($4 \times 10^{-21} \text{ cm}^2$),⁵ thus no order of magnitude increase of σ_{abs} due to the presence of the Si-nc is observed as claimed in Ref. 7 (claims revised in Ref. 9). Figure 2 reports the absorption and emission cross section spectra (σ_{em}) for all the investigated waveguide samples. σ_{em} is deduced from the PL spectra at low pumping rates (see later). Both σ_{abs} and σ_{em} spectral line shapes change with varying the annealing time. This has been inter-

preted as a change in the interaction of Er³⁺ with the field of the embedding medium (local field effects). Here, we do not detail the physics behind but we simply notice that the internal transitions of Er³⁺ are affected by the annealing time.

In Table I, α_{abs} is reported for the various waveguides as a function of n . Figure 3(a) shows the decreasing of σ_{abs} with increasing n . As a completion of the absorption measurements, because of the relation between cross sections and lifetimes (τ), we performed lifetime measurements: Single exponential decay curves have been found. The results are shown in Fig. 3(b): τ increases from 2.3 to 3.8 ms in the waveguide samples annealed for 10 and 60 min, respectively. At first sight, these results seem to contradict other experimental findings of an increase in the transition rate when the refractive index of the material increases.¹⁵ However, this is true when the emission/absorption cross section of Er³⁺ is constant, i.e., when only mean-field corrections are applied due to dielectric composition variations which lead to a change in n .

As we already stated, in our waveguides, we observed both a variation of the average composition (which is reflected in a variation of n) and a variation of the local field (which is reflected in a lineshape variation of the Er related optical transitions). This can be inferred by using the following equation:¹⁵

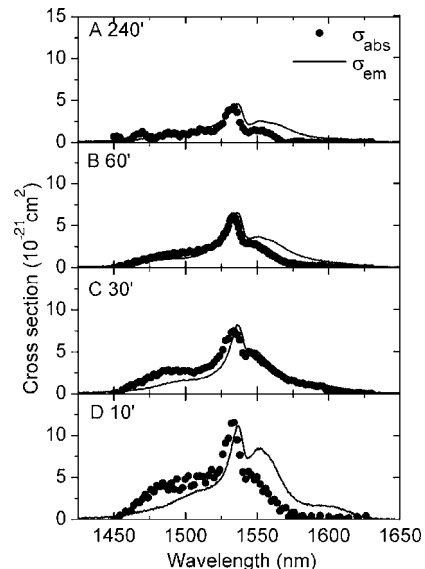


FIG. 2. Absorption (disks) and emission (lines) cross section spectra for the different waveguides. The various panels are labeled with the waveguide sample names and the annealing times. Emission cross sections are obtained from low pump power ($1 \times 10^{18} \text{ ph/s cm}^2$) PL spectra excited at 488 nm by normalizing the PL maximum to the maximum of the absorption cross section, [i.e., by using Eq. (2)].

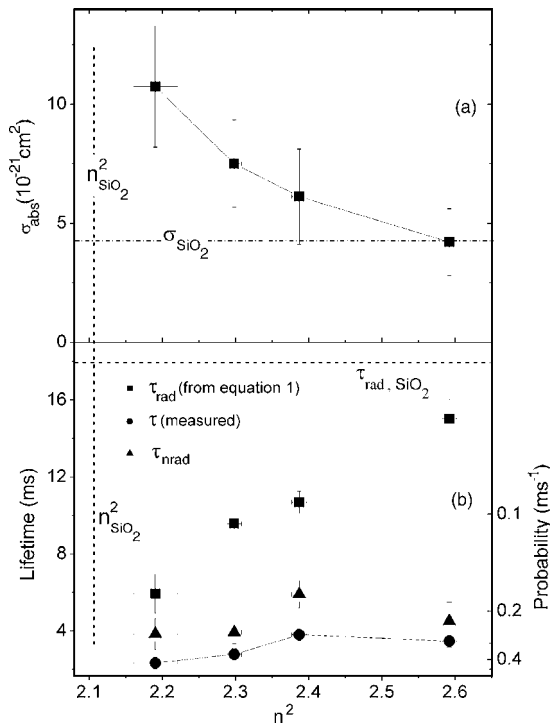


FIG. 3. (a) Absorption cross section at 1534 nm as a function of the square of the refractive index n . (b) Measured (disks), radiative (squares), and nonradiative (triangles) lifetimes as a function of the square of the refractive index n . Total lifetimes at 1535 nm have been measured at 488 nm at low photon flux (1×10^{18} ph/s cm^2) [while the rest have been calculated using Eq. (1)]. Data for Er^{3+} in SiO_2 taken from the literature (Refs. 5 and 17) are also plotted as straight lines.

$$\frac{1}{\tau_{\text{rad}}} = \frac{8\pi n^2}{c^2} \int \nu^2 \sigma_{\text{em}}(\nu) d\nu, \quad (1)$$

where

$$\sigma_{\text{em}}(\nu) = \sigma_{\text{abs}}(\nu) e^{\frac{\varepsilon - h\nu}{kT}}. \quad (2)$$

In Eq. (2), ε is a parameter. Equation (1) shows that what is changing when n is varied is the ratio between the radiative recombination rate and the integrated σ_{em} . In order to obtain σ_{em} , we have normalized the PL spectra at low pump power to the maximum value of σ_{abs} for each waveguide, by supposing that σ_{abs} and σ_{em} are equal at maximum. Then from Eq. (1), we can deduce τ_{rad} . Finally, from τ and τ_{rad} , we can calculate the nonradiative lifetimes (τ_{nrad}). All these values are shown in Fig. 3(b). The relevance of local field effects is clearly evidenced as τ_{rad} is increasing as a function of n^2 . It is interesting that on waveguide sample A, which is completely phase separated and the dielectrics has high quality, we have obtained a τ_{rad} which is smaller than the literature value for Er in pure silica. This can be explained in terms of mean field variations (larger n).

What has been previously shown,¹⁶ i.e., the increase of the decay rate of Er^{3+} as a function of n of the embedding medium, is consistent with the results of the present letter when variations in the mean field and not in the local field are considered. The reduction of σ_{abs} with annealing time [Fig. 3(a)] is due to the change of the Er^{3+} environment, which is changing from a SRO to a two-phase (Si-nc and SiO_2) system. Since Er^{3+} is in the oxide, as the phase separation

progresses Er^{3+} is surrounded more and more by a pure SiO_2 environment. Consequently, σ_{abs} tends to the value for Er^{3+} in pure silica.¹⁷

Finally, it has to be remarked that the σ_{abs} evaluation requires an estimate of the optical mode confinement factor Γ . This does not yield to an inaccurate σ_{abs} , once Γ is correctly calculated or measured. In fact, for two different etching procedures of the same waveguide sample D which results in different Γ (see Table I), we found σ_{abs} values of $11 \pm 4 \times 10^{-20}$ and $14 \pm 5 \times 10^{-20}$ cm^2 , respectively, which are the same within the error bars.

In conclusion, we have measured the Er^{3+} absorption cross section σ_{abs} and lifetimes at 1.54 μm in silicon-rich oxide waveguides where Si-nc are forming. No dramatic enhancement of σ_{abs} has been found with respect to the values typical of Er in SiO_2 . However, a decrease of the absorption cross section as a function of the annealing time has been pointed out and explained in terms of the sum of the mean and local field effects on the Er^{3+} transitions. Moreover, cross sections and radiative lifetimes for the ${}^4I_{13/2} \rightarrow {}^4I_{15/2}$ transition tend to the values found in literature for Er^{3+} in SiO_2 when a compact and defect-free SiO_2 dielectric is formed for long annealing time. These findings fix some ambiguous issues concerning the absorption cross section of Er^{3+} in Si-nc waveguides thus allowing correct modeling of gain in such systems.

This work has been supported by EC through the SIN-ERGIA project and FIRB. The authors acknowledge L. Cognolato from Agilent (Torino) and G. Pucker from ITC-IRST (Trento) for waveguide processing, B. Garrido and C. Garcia from University of Barcelona, and E. Borsella from ENEA (Frascati - Roma) for scientific discussions.

¹D. Pacifici, G. Franzò, F. Priolo, F. Iacona, and L. Dal Negro, Phys. Rev. B **67**, 245301 (2003).

²A. Polman and F. C. J. M. van Veggel, J. Opt. Soc. Am. B **21**, 871 (2004).

³J. Lee, J. H. Shin, and N. Park, J. Lightwave Technol. **23**, 19 (2005).

⁴D. Kovalev, J. Diener, H. Heckler, G. Polisski, N. Künzer, and F. Koch, Phys. Rev. B **61**, 4485 (2000).

⁵W. J. Miniscalco, J. Lightwave Technol. **9**, 234 (1991).

⁶S. Lombardo, S. U. Campisano, G. N. van den Hoven, A. Cacciato, and A. Polman, Appl. Phys. Lett. **63**, 1942 (1993).

⁷P. G. Kik, A. Polman, J. Appl. Phys. **91**, 534 (2002).

⁸H. S. Han, S. Y. Seo, J. H. Shin, and N. Park, Appl. Phys. Lett. **81**, 3720 (2002).

⁹H. Mertens, A. Polmann, I. M. P. Aarts, W. M. M. Kessels, and M. C. M. van de Sanden, Appl. Phys. Lett. **86**, 241109 (2005).

¹⁰N. Daldosso, D. Navarro-Urrios, M. Melchiorri, L. Pavesi, F. Gourbilleau, M. Carrada, R. Rizk, C. Garcia, P. Pellegrino, B. Garrido, and L. Cognolato, Appl. Phys. Lett. **86**, 261103 (2005).

¹¹F. Gourbilleau, C. Dufour, M. Levalois, J. Vicens, R. Rizk, C. Sada, F. Enrichi, and G. Battaglin, J. Appl. Phys. **94**, 3869 (2003).

¹²F. Gourbilleau, M. Levalois, C. Dufour, J. Vicens, and R. Rizk, J. Appl. Phys. **95**, 3717 (2004).

¹³J. A. Moreno, B. Garrido, P. Pellegrino, C. Garcia, J. Arbiol, K. R. Morante, P. Marie, F. Gourbilleau, and R. Rizk, J. Appl. Phys. **98**, 013523 (2005).

¹⁴N. Daldosso, D. Navarro-Urrios, M. Melchiorri, C. Garcia, P. Pellegrino, B. Garrido, C. Sada, G. Battaglin, F. Gourbilleau, R. Rizk, and L. Pavesi (unpublished).

¹⁵W. J. Miniscalco and R. S. Quimby, Opt. Lett. **16**, 258 (1991).

¹⁶E. Snoeks, A. Lagendijk, and A. Polman, Phys. Rev. Lett. **74**, 2459 (1995).

¹⁷M. J. A. de Dood, L. H. Slooff, A. Polman, A. Moroz, and A. van Blaaderen, Phys. Rev. A **64**, 033807 (2001).